LEAVE THIS PAGE BLANK
DO NOT DELETE THIS PAGE

Functionally Graded Architectural Materials

Integrated and Tailored Thermal Insulation through Gradient Multimaterial Additive Manufacturing for Masonry Architectural Components

Teng Teng
University of Pennsylvania
Yefan Zhi
University of Pennsylvania
Masoud Akbarzadeh
University of Pennsylvania

1

1 Detailed shot of the fabrication experiment, imagining the multi-material thermal-insulated wall system applied on larger scales.

ABSTRACT

Achieving Integrated Tailored Thermal Insulation (ITTI) for architectural components can enhance building energy efficiency. However, it presents significant technical challenges. This paper introduces an approach using gradient multimaterial additive manufacturing (MMAM) to overcome these challenges. We adopt the Single-Nozzle system to process paste and filament materials, including clay/diatomite-based and fiber-fused/foaming polyethylene filament, to achieve seamless material transitions and optimized thermal properties. Initial validation involves testing for print quality and functionality. Subsequently, we fabricate a series of polyethylene masonry units to form a wall system, where high-stress regions are reinforced with fiber-fused polyethylene while low-stress areas are composed of foaming polyethylene, providing both load- bearing capacity and thermal insulation. Results indicate significant improvements in printability, structural integrity, and thermal efficiency of the printed components.

Keywords: *multimaterial additive manufacturing, functionally graded material, architectural insulation, load-bearing, 3d printing*

INTRODUCTION

Masonry structures and its insulation

Contemporary masonry architecture often employs a layered approach for load-bearing structures and insulation, treating them as separate components of the building envelope (Frampton 2001). While this method is widely used, it poses challenges for thermal efficiency.

Masonry relies on durable materials like concrete blocks, bricks, and stone for structural loads (Hendry 2001). These materials are arranged in bonding patterns such as running bond, stack bond, or Flemish bond, with mortar providing both adhesion and load distribution to enhance stability.

Thermal insulation is typically added as a separate layer, using materials like rigid foam boards, fiberglass batts, or spray foam (Bojić and Loveday 1997; Orlik-Kożdoń 2019). These are applied to the wall's interior or exterior, with rigid foam or fiberglass batts installed within framing systems, and spray foam filling gaps to improve thermal performance.

Thermal bridging, identified by Orlik-Kożdoń (2019), occurs when structural elements such as concrete blocks and mortar joints interrupt insulation, allowing heat transfer and reducing efficiency. Additionally, the separation between load-bearing and insulation layers complicates construction, as materials expand differently under extreme conditions, risking delamination and structural integrity (Sridharan 2008). This increases labor demands and installation complexity.

Integrated Tailored Thermal Insulation

To address the thermal insulation challenges in masonry architecture, we propose Integrated and Tailored Thermal Insulation (ITTI) (Figure 2) as a solution to mitigate thermal bridging and the separation between load-bearing and insulating elements.

ITTI integrates insulation directly into structural components, eliminating separate layers. This approach uses multimaterial additive manufacturing (MMAM) to tailor material composition within a single component, allowing a gradual transition from structurally strong areas to insulated zones. By precisely controlling material distribution, ITTI optimizes thermal performance and structural integrity.

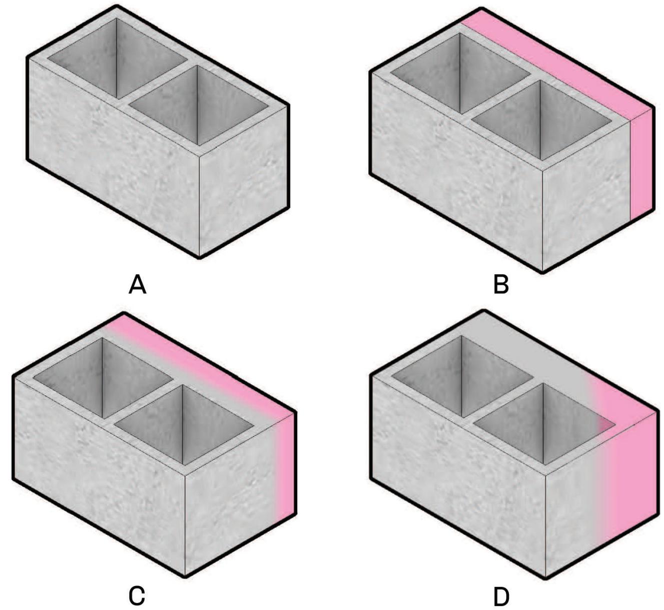

2

2 An introduction of Integrated Tailored Thermal Insulation. (A) a conventional concrete cinder block commonly used as a load-bearing component in architectural systems; (B) a conventional method of assembling load-bearing structure and insulation layer together; (C) the integrated insulation method that the insulation material seamlessly transits to load-bearing component; and (D) the proposed Integrated Tailored Thermal Insulation method that transitional material distribution can be tailored based on design demand.

3 A diagram showing the two types of material suppliers with the single-nozzle Multimaterial (SNMM) extruder system on a modified 3d printer gantry:

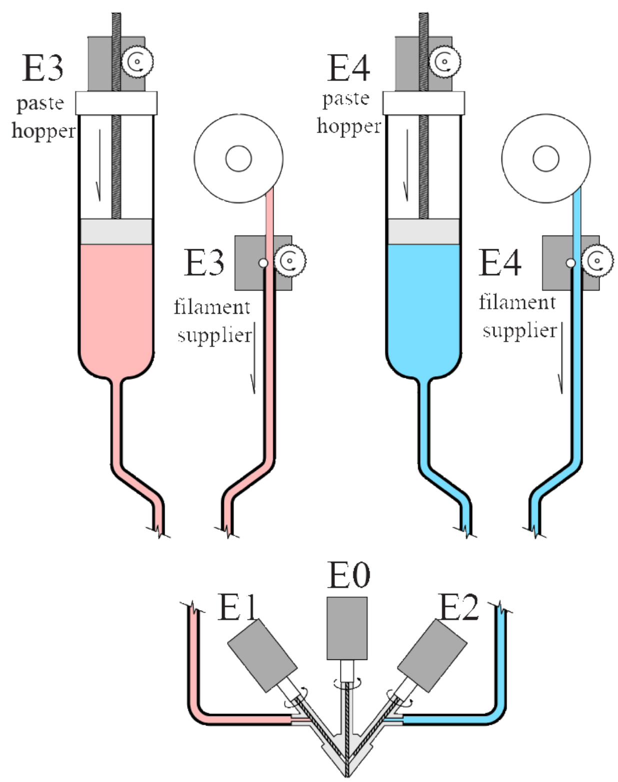

3

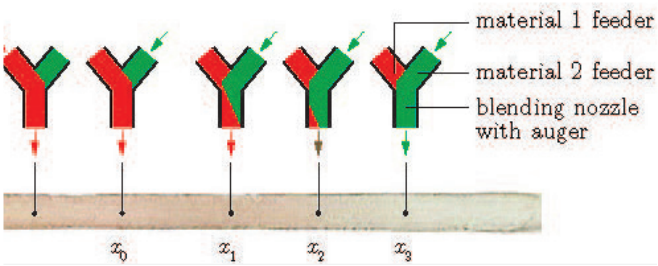

4

5

4 A printing test showing the material transitional behavior. In this printing test, the motor is instructed to switch from material 1 to material 2 at x0. However, the resulting actual interface is observed to be at x2. Therefore the printing advancement length can be determined as L = x2 – x0.

5 Material transition tests. Print results of 2D zig-zag toolpaths with no advancement (left) and advancement length L = 58 mm (right);

This integration eliminates interfaces that cause thermal bridging, improving thermal efficiency and energy performance. It also streamlines construction by reducing the need for multiple layers, enhancing overall component integrity. ITTI advances masonry design, making buildings more sustainable and efficient.

However, ITTI faces manufacturing challenges, particularly in achieving smooth material transitions between load-bearing and insulating materials. This requires advanced equipment and precise material deposition.

MMAM technologies offer potential for seamless material transitions, but their complexity limits broader adoption in construction. Extrusion-based MMAM is a promising, scalable option, though further research is needed to address current limitations.

This paper reviews precedent works and presents material and printing tests to establish a process for producing functional architectural components using ITTI.

State of the Art

The precedent works are reviewed in three areas: multi-material additive manufacturing (MMAM) for architecture,

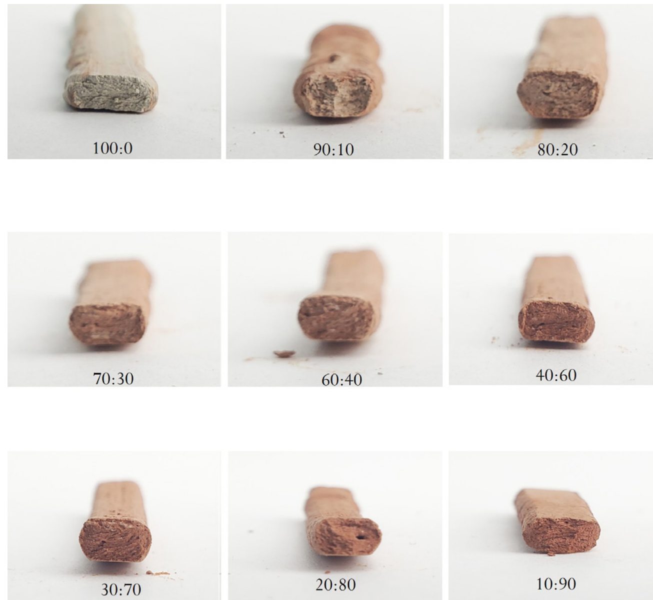

6

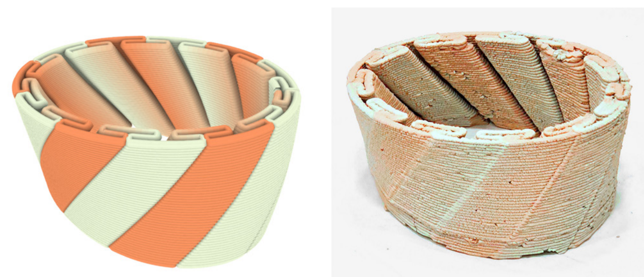

7

6 Material composition control through the SNMM extruder system.

7 Visualization (left) and printing results (right) of the multimaterial toolpath of a cylindrical geometry with red and green clays where the transitional segments are folded and hidden.

novel construction paste materials, and thermal performance improvements for masonry components.

In MMAM, two extrusion setups dominate: multi-nozzle and single-nozzle. Multi-nozzle systems, known for ease of assembly (Darnal et al. 2023; Dutto et al. 2023; Ali, Mir-Nasiri, and Ko 2016; Khalil et al. 2004; Skylar-Scott et al. 2019), can struggle with weak material bonding at interfaces (Yin et al. 2018) and require frequent calibration (Inamdar et al. 2006; Sodupe-Ortega et al. 2018; Kolesky et al. 2014). Seibold et al. (2019) introduced a dual-chamber printhead for ceramic manufacturing, improving masonry insulation but facing limitations in complexity, material compatibility, and scalability. Single-nozzle systems, using continuous extrusion, improve material bonding and performance (Baca and Ahmad 2020), especially in microfluidics and fused filament fabrication (Song et al. 2019;

Fenollosa et al. 2021). Active mixing, originating from microfluidics (Nguyen and Wu 2004), allows precise control of material composition and gradient transitions (Ren et al. 2018).

For mid- and large-scale MMAM, Craveiro et al. (2018, 2020) explored cement mixtures with cork granules, enhancing insulation but limiting structural integrity and scalability. Chee et al. (2018) used digitally controlled injection in concrete to customize properties but faced scalability challenges. Dutto et al. (2023) examined wet foam for 3D printing porous ceramics, but issues with foam control and scalability persist.

Jauk et al. (2023) used multimaterial coextrusion to achieve functionally graded porosity in ceramics, but scalability and material compatibility remain challenges. Ma et al. (2022) integrated aerogels into concrete for insulation, reducing strength, while Dal et al. (2020) explored diatomite-based firebricks for industrial insulation but noted scalability issues. Martínez-Díez et al. (2001) found that polyethylene foam blocks have higher thermal conductivity in central regions due to cell size variations. Sun et al. (2021) identified thermal bridging in 3D printed concrete buildings, emphasizing the need for optimized material formulations.

Ismaiel et al. (2022) reviewed strategies to enhance masonry wall thermal resistance, recommending improved design, manufacturing, and material use, such as tight insulation contact and thermal break assemblies, but these require interdisciplinary collaboration.

METHODOLOGY

This section outlines the system setup, material compatibility tests, printability tests, and design methods for producing functional ITTI products.

System Setup

We developed an incremental, multi-step process using a Single-Nozzle Multimaterial (SNMM) extruder system(Figure 3). This system features a single nozzle with a blending auger (E0) for mixing materials, feeding augers (E1, E2) for controlling material flow, and material suppliers (E3, E4) (Figure 4A). The SNMM extruder, attached to a modified Creality CR10-MAX printer, can handle up to two different materials with a large print volume (500mm^3). It employs eight stepper motors for control, using a custom PCB for precise regulation. The setup accommodates high-viscosity materials like clay and concrete, with a 4mm nozzle diameter and 10mm PVC hoses for high-pressure extrusion.

System Control

Mixing two paste-like materials poses challenges due to differing viscosities (Rafiee et al. 2020), which can cause inconsistent flow or blockages. The SNMM system, controlled by our custom PCB, adjusts motor speeds to regulate material composition. Additives were tested to improve pumpability, extrudability, load-bearing capacity, and thermal conductivity. We tested two combinations: clay with diatomite paste, and fiber-fused polyethylene with foaming lightweight polyethylene (PLA). Both materials offer high printability and are free from large aggregates.

Material Transitional Behavior

Smooth material transitions are crucial in single-nozzle printing. The system switches between materials by altering motor speeds, ensuring a gradient transition (Figure 4). Our GCode controls material switches based on extrusion speed, avoiding distinct material interfaces by adjusting the motor-switch command in advance. A test using two clay bodies demonstrated that advancing the motor switch by 58mm significantly improved print quality (Figure 5).

Composition Control

The SNMM system can blend materials by adjusting the rotational speed ratio between feeding augers. In one test, red earthenware clay and white diatomite paste were blended in varying proportions, creating a gradient from 100% diatomite to 100% earthenware (Figure 6). The new mixture contains from 100% to 0% of diatomite paste (mat1) and 0% to 100% of earthenware clay (mat2):

$$\mathbf{P} = \begin{array}{c} \\ \text{mix}_1 \\ \text{mix}_2 \\ \text{mix}_3 \\ \text{mix}_4 \\ \text{mix}_5 \\ \text{mix}_6 \\ \text{mix}_7 \\ \text{mix}_8 \\ \text{mix}_9 \\ \text{mix}_{10} \end{array} \begin{array}{c} \begin{array}{cc} \text{mat}_1 & \text{mat}_2 \end{array} \\ \begin{pmatrix} 1 & 0 \\ 0.9 & 0.1 \\ 0.8 & 0.2 \\ 0.7 & 0.3 \\ 0.6 & 0.4 \\ 0.4 & 0.6 \\ 0.3 & 0.7 \\ 0.2 & 0.8 \\ 0.1 & 0.9 \\ 0 & 1 \end{pmatrix} \end{array}$$

Multimaterial Visualization

To visualize toolpaths in multimaterial printing, we used vertex coloring to reflect material composition, predicting the final print's gradient transitions (Figure 8).

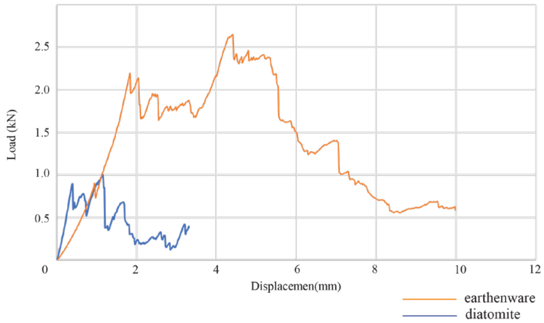

8

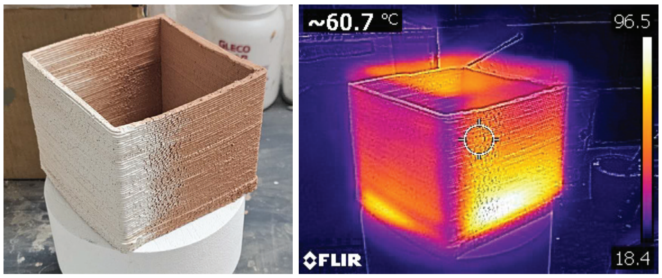

9

8 Compressive test result of earthenware and diatomite cylinder samples.

9 The printed cubic geometry with red earthenware and diatomite (left); IR photo taken by thermal camera indicating the differences of thermal performance within one continue object (right).

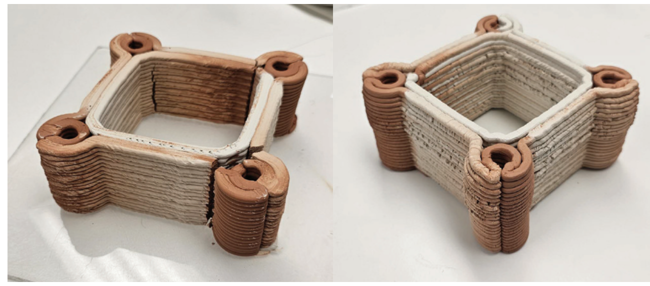

10

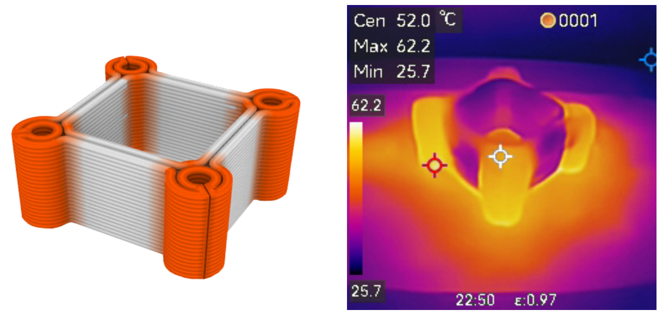

11

10 Multimaterial printing tests: Right, the test group with hydroxypropyl methylcellulose applied; and Left, the control group without hydroxypropyl methylcellulose.

11 The visuliatzion of the geometrical design; IR photo of the printed piece indicating the differences of thermal performance within one continue object when set in the heated envionment.

Material Compatibility and Functional Tests

We studied two material combinations: clay/diatomite paste and fiber-fused polyethylene/foaming polyethylene. Diatomite and foaming polyethylene are highly porous, ideal for thermal insulation (Ivanov and Belyakov 2008; Nofar and Park 2014), while clay provides load-bearing capabilities. To ensure compatibility, we added hydroxypropyl methylcellulose to diatomite paste, preventing cracks during drying (Figure 9 and 10). Compression tests revealed that clay cylinders can support up to 2.7 kN, while diatomite cylinders support 1 kN (Figure 8). An IR photo confirmed the thermal properties, with diatomite absorbing less heat than earthenware in a kiln test (Figure 9 and 11).

For fiber-fused and foaming polyethylene, we determined an optimal motor speed ratio of 6.67:1 and set the temperature 10% lower than PLA's to avoid overswelling.

As a pilot study, we used our SNMM system to print two classical paintings, the Mona Lisa and the Girl With Pearl Earrings, using carbon fiber-fused PLA and foaming PLA. As Figure 12 demonstrated, the printing results show high fidelity and reflect the original appearance of both paintings. As foaming PLA is highly porous, thus its thermal conductivity is lower than carbon fiber-fused PLA. Therefore, we placed both printed pieces in a climate chamber, set the ambient temperature at 60°C for 30 minutes, and used a thermal camera to verify that the material change within the piece would reflect the thermal situation.

The IR photos of both pieces exhibited the original graph, indicating the heat absorption varies due to the material change.

RESULT

This section presents a case study using the developed SNMM system, printing parameters, and material data to further demonstrate the feasibility and effectiveness of the proposed Integrated and Tailored Thermal Insulation.

We designed a masonry wall piece utilizing computational tools for optimal structural and thermal performance. The process begins with stress analysis using Karamba3D in Grasshopper3D, where six vertical loads are applied to the top of the wall, supported by two base points (Figure 13A). The analysis identifies principal stress lines:blue for compression and red for tension (Figure 13B). Based on these stress patterns, the wall's rib structure is generated (Figure 13C). Fiber-fused PLA is placed in high-compression areas for enhanced load-bearing, while foaming PLA is used in non-load-bearing areas and for insulation (Figure 13D). The wall is then divided into printable sections with slicing planes defined for orientation (Figure 13E and F).

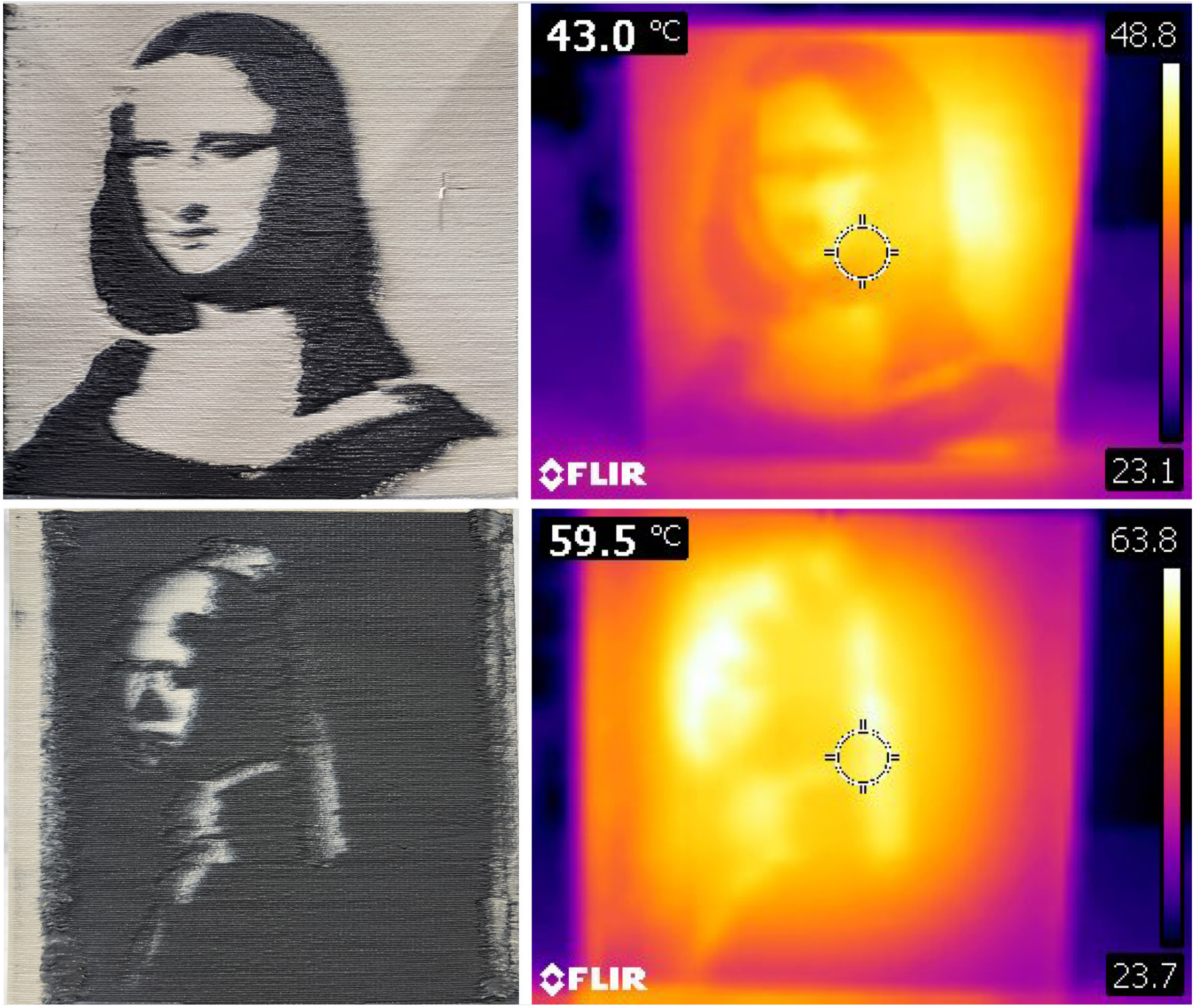

12

12 The Mona Lisa and a girl with pearl earrings printed with carbon fiber fused PLA filament and foaming PLA filament(left); the IR photo of the printed piece showing the surface temperature is differentiated in different material regions(right).

This approach ensures each component is optimized for its structural and functional roles, resulting in a 3D-printable, multi-functional masonry wall.

The toolpath design for the masonry wall system is critical to achieving both structural integrity and thermal efficiency. The process starts by identifying the wall's load-bearing components (Figure 14A). For efficient 3D printing, continuous curves are developed as toolpaths. This involves offsetting the rib profile and creating folds in the load-bearing areas, adding mass to compression zones for increased strength (Figure 14B and C). Each masonry piece features more folds in the load-bearing regions and is printed with fiber-fused PLA. The remaining areas, shown in white, are printed with foaming PLA for insulation (Figure 14D). The seamless transition between the two materials ensures optimal performance without distinct material interactions. This method results in a masonry wall piece optimized for both load-bearing capacity and thermal insulation, with an efficient, continuous toolpath to streamline the printing process.

After designing and slicing the masonry wall system, we fabricated all masonry units using our SNMM printer with fiber-fused and foaming PLA (Figure 15).

The masonry wall system (Figures 15 and 16), produced with a single-nozzle multimaterial 3D printer, shows significant thermal performance. After one hour of direct sunlight exposure at 32°C, thermal imaging (Figure 17) highlights

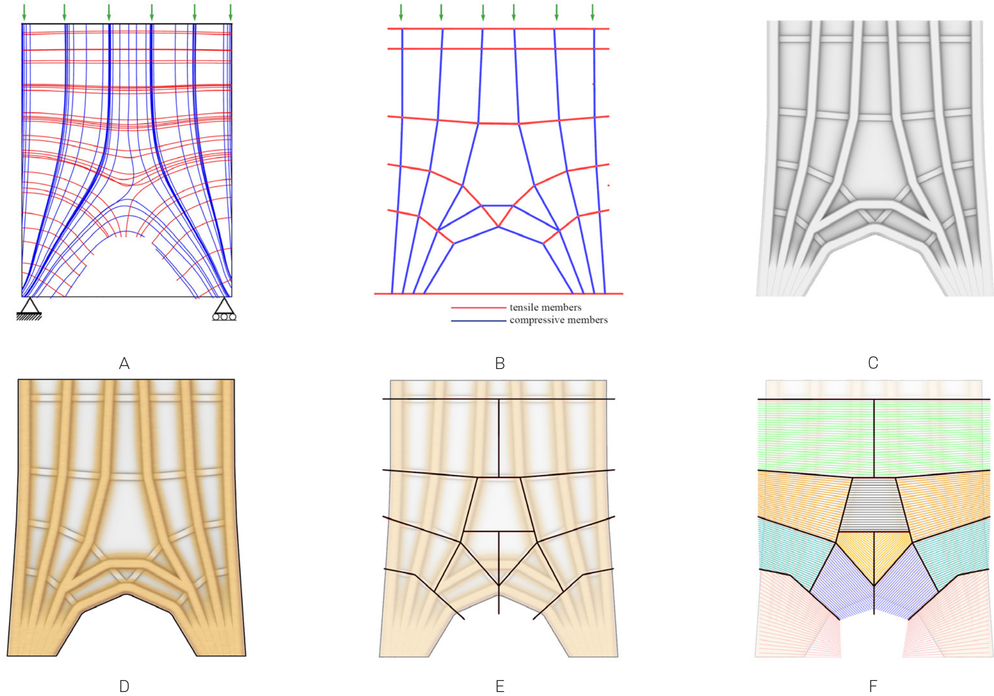

13

13 The design process of the wall system: (A) The initial stress analysis of the wall geometry using Karamba3D in Grasshopper3D. Six vertical loads are applied at the top of the wall, and two supports are positioned at the base. (B) The identified principal stress lines: blue lines indicate regions of concentrated compressive stress, while red lines indicate regions of tensile stress. These lines inform the subsequent structural design of the wall. (C) The generated rib structure of the wall is based on the principal stress lines. (D) The application of materials based on stress regions: stronger material (shown in yellow) is used in compression regions for load-bearing purposes, while insulation material (shown in white)is applied in other regions for thermal insulation. (E) The division of the wall piece for fabrication. This step involves breaking down the wall into manageable sections, ensuring ease of production and assembly. (F) Definition of slicing planes based on the division

distinct thermal behavior between the materials. The exterior, composed of both fiber-fused PLA in load-bearing areas and foaming PLA for insulation, reveals that the fiber-fused PLA absorbs more heat, while the foaming PLA remains cooler.

The interior side, which is fully made of foaming PLA and not exposed to direct sunlight, maintains much lower temperatures, indicating strong thermal insulation. The seamless transition between materials ensures no distinct interaction between them, effectively balancing structural support and insulation. These findings validate the concept of Integrated and Tailored Thermal Insulation, demonstrating that combining fiber-fused PLA for structural strength and foaming PLA for insulation efficiently meets both thermal and structural requirements.

CONCLUSION

This study demonstrated the effectiveness of gradient multimaterial additive manufacturing (MMAM) in improving the thermal and structural performance of masonry wall systems. By using a single-nozzle multimaterial (SNMM) 3D printing system, we achieved seamless transitions between load-bearing and insulating materials, addressing challenges like thermal bridging and structural integrity in conventional masonry.

Computational tools, such as Karamba3D in Grasshopper3D, enabled stress analysis to guide material placement. Fiber-fused PLA was used in high-stress areas for load-bearing, while foaming PLA provided thermal insulation in low-stress zones, optimizing material use while maintaining structural integrity and thermal efficiency.

Thermal performance tests under direct sunlight confirmed the approach. Load-bearing regions with fiber-fused PLA absorbed more heat, while insulating areas with foaming PLA stayed cooler. The interior side, shielded from sunlight, remained significantly cooler, highlighting effective thermal insulation. Smooth transitions between materials ensured consistent thermal performance.

These results highlight the potential of MMAM for creating functionally graded masonry components that meet both structural and thermal needs. This approach enhances energy efficiency and simplifies construction by reducing the need for multiple layers. Future research should focus on optimizing materials and printing strategies to improve scalability and practical application.

REFERENCES

Ali, Md Hazrat, Nazim Mir-Nasiri, and Wai Lun Ko. 2016. "Multi-nozzle extrusion system for 3D printer and its control mechanism." The International Journal of Advanced Manufacturing Technology 86:999–1010.

Baca, David, and Rafiq Ahmad. 2020. "The impact on the mechanical properties of multi-material polymers fabricated with a single mixing nozzle and multi-nozzle systems via fused deposition modeling." The International Journal of Advanced Manufacturing Technology 106 (9-10): 4509–4520.

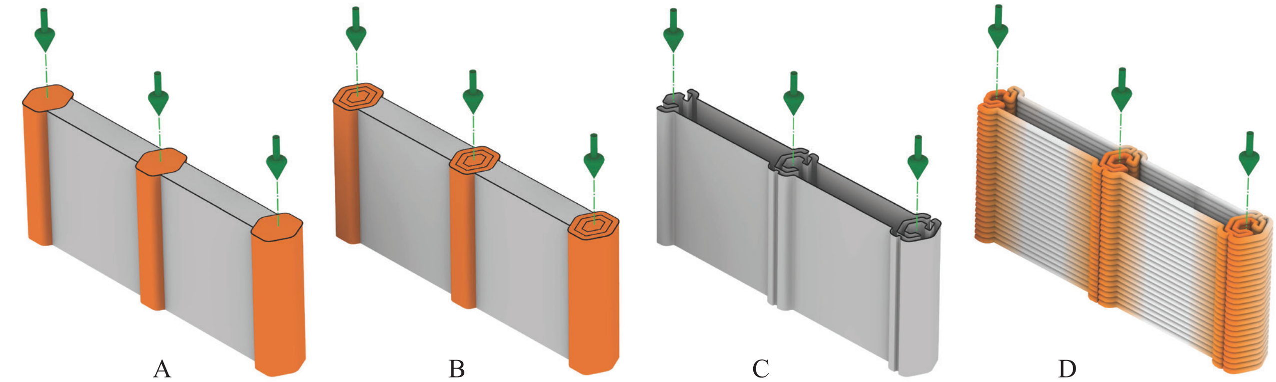

14 A generalizable toolpath design method for wall system: (A) Initial configuration of the wall section with identified load-bearing components. The load-bearing regions, shown in orange, are designed to absorb vertical loads, indicated by red arrows. (B) Offset profile generation for the load-bearing components. This process adds folds within these regions, increasing the material mass in compression areas to ensure enhanced structural strength. (C) Illustration of the toolpath design as a continuous curve. (D) The final wall component shows the seamless transition between fiber-fused PLA (in orange) for load-bearing regions and foaming PLA (in white) for insulation. The transition between the materials prevents any distinct interaction between the different materials and maintains the structural and thermal integrity of the wall. 14

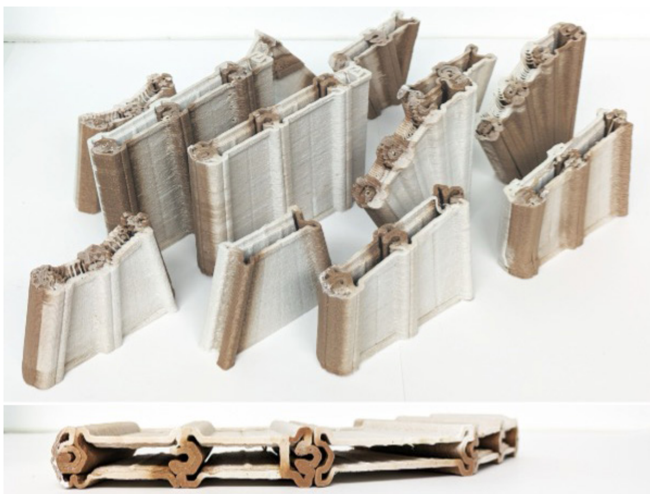

15

16

Bojić, M Lj, and DL Loveday. 1997. "The influence on building thermal behavior of the insulation/masonry distribution in a three-layered construction." Energy and buildings 26 (2): 153–157.

Chee, RW, WL Tan, WHG Goh, F Amtsberg, and S Dritsas. 2018. "Locally differentiated concrete by digitally controlled injection." In Learning, Adapting and Prototyping-Proceedings of the 23rd CAADRIA Conference. Tsinghua University, Beijing, China, 195–204.

Craveiro, Flávio, Helena Bártolo, Paulo Bártolo, Shadi Nazarian, and Jose Duarte. 2018. "Additive manufacturing of functionally graded building parts: towards seamless architecture." In 4th Biennial Residential Building Design & Construction Conference Proceedings, 529–540.

Craveiro, Flávio, Shadi Nazarian, Helena Bartolo, Paulo Jorge Bartolo, and José Pinto Duarte. 2020. "An automated system for 3D printing functionally graded concrete-based materials." Additive Manufacturing 33:101146.

Dal, Serkan, Mucahit Sutcu, Mustafa Sabri Gok, and Osman Gencel. 2020. "Characteristics of lightweight diatomite-based insulating firebricks." Journal of the Korean Ceramic Society 57 (2): 184–191.

Darnal, Aryabhat, Zaryab Shahid, Himani Deshpande, Jeeeun Kim, and Anastasia Muliana. 2023. "Tuning mechanical properties of 3D printed composites with PLA: TPU programmable filaments." Composite Structures 318:117075.

Dutto, Alessandro, Michele Zanini, Etienne Jeoffroy, Elena Tervoort, Saurabh A Mhatre, Zachary B Seibold, Martin Bechthold, and André R Studart. 2023. "3D printing of hierarchical porous ceramics for thermal insulation and evaporative cooling." Advanced Materials Technologies 8 (4): 2201109.

16

15 Details of printed wall pieces: The printing process utilizes a non-parallel printing approach, and the slicing plans approximately follow the tension direction. Horizontal adjacent units are designed with joint slots.

Federowicz, Karol, Maria Kaszyńska, Adam Zieliński, and Marcin Hoffmann. 2020. "Effect of curing methods on shrinkage development in 3D-printed concrete." Materials 13 (11): 2590.

Fenollosa, F, R Uceda, A Tejo, L Calvo, Louison Poudelet, and I Buj. 2021. "Research on desktop 3D Printing Multi-Material New Concepts." In IOP Conference Series: Materials Science and Engineering, 1193:012043. 1. IOP Publishing.

Frampton, Kenneth. 2001. Studies in tectonic culture: the poetics of construction in nineteenth and twentieth century architecture. Mit Press.

Hendry, AW. 2001. "Masonry walls: materials and construction." Construction and Building materials 15 (8): 323–330.

Inamdar, Asim, Marco Magana, Frank Medina, Yinko Grajeda, and Ryan Wicker. 2006. "Development of an automated multiple material stereolithography machine." In 2006 International Solid Freeform Fabrication Symposium.

Ismaiel, Maysoun, Yuxiang Chen, Carlos Cruz-Noguez, and Mark Hagel. 2022. "Thermal resistance of masonry walls: a literature review on influence factors, evaluation, and improvement." Journal of Building Physics 45 (4): 528–567.

Ivanov, S É, and AV Belyakov. 2008. "Diatomite and its applications." Glass & Ceramics 65.

Jauk, Julian, Hana Vašatko, Lukas Gosch, Kristijan Ristoski, Josef Füssl, and Milena Stavric. 2023. "Coextrusion of Clay-Based Composites: Using a Multi-Material Approach to Achieve Gradient Porosity in 3D-Printed Ceramics." Ceramics 6 (4): 2243–2255.

Jo, Jun Ho, Byung Wan Jo, Woohyun Cho, and Jung-Hoon Kim. 2020. "Development of a 3D printer for concrete structures: laboratory testing of cementitious materials." International Journal of Concrete Structures and Materials 14:1–11.

Khalil, S, J Nam, A Darling, and W Sun. 2004. "Multi-nozzle biopolymer deposition for freeform fabrication of tissue constructs." In 2004 International Solid Freeform Fabrication Symposium.

Kolesky, David B, Ryan L Truby, A Sydney Gladman, Travis A Busbee, Kimberly A Homan, and Jennifer A Lewis. 2014. "3D bioprinting of vascularized, heterogeneous cell-laden tissue constructs." Advanced materials 26 (19): 3124–3130.

Ma, Guowei, A Ruhan, Panpan Xie, Zhu Pan, Li Wang, and James C Hower. 2022. "3D-printable aerogel- incorporated concrete: Anisotropy influence on physical, mechanical, and thermal insulation properties." Construction and Building Materials 323:126551.

Martínez-Díez, JA, MA Rodríguez-Pérez, JA De Saja, LO Arcos y Rábago, and OA Almanza. 2001. "The thermal conductivity of a polyethylene foam block produced by a compression molding process." Journal of cellular plastics 37 (1): 21–42.

Nguyen, Nam-Trung, and Zhigang Wu. 2004. "Micromixers—a review." Journal of micromechanics and microengineering 15 (2): R1.

Nofar, Mohammadreza, and Chul B Park. 2014. "Poly (lactic acid) foaming." Progress in Polymer Science 39 (10): 1721–1741.

Orlik-Kożdoń, Bożena. 2019. "Interior insulation of masonry walls—selected problems in the design." Energies 12 (20): 3895.

Ortega, Jason M, Melody Golobic, John D Sain, Jeremy M Lenhardt, Amanda S Wu, Scott E Fisher, Lemuel X Perez Perez, Adam W Jaycox, James E Smay, Eric B Duoss, et al. 2019. "Active mixing of disparate inks for multimaterial 3D printing." Advanced Materials Technologies 4 (7): 1800717.

Rafiee, Mohammad, Rouhollah D Farahani, and Daniel Therriault. 2020. "Multi-material 3D and 4D printing: a survey." Advanced Science 7 (12): 1902307

.

Ren, Luquan, Zhengyi Song, Huili Liu, Qinghe Han, Che Zhao, Brian Derby, Qingping Liu, and Lei Ren. 2018. "3D printing of materials with spatially non-linearly varying properties." Materials & Design

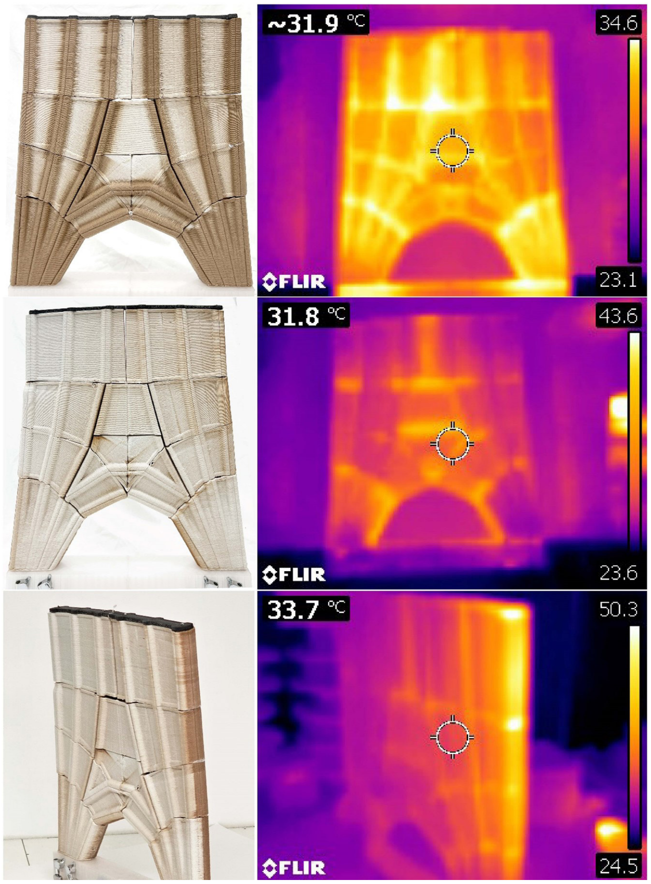

17

16 Top Row: Exterior Side of the Wall. Left Image: The exterior side of the wall, printed with a combination of fiber-fused filament and foaming PLA. Right Image (IR): Thermal image taken after one hour of direct sunlight exposure (32°C), showing heat absorption by the fiber-fused filament. Middle Row: Interior Side of the Wall. Left Image: The interior side of the wall, not directly exposed to sunlight. Right Image (IR): IR image showing that the interior side remains significantly cooler compared to the exterior side. Bottom Row: Left Image: Close-up of the transition area between the exterior and interior sides of the wall. Right Image (IR): Thermal image of the transition area, confirming a smooth material transition with consistent thermal properties and no distinct interactions.

156:470–479.

Seibold, Zach, Saurabh Mhatre, Suleiman Alhadidi, Jose Luis García del Castillo y López, and Martin Bechthold. 2019. "Janus Printing: Coextrusion based Multi-material Additive Manufacturing for Ceramics." In Proceedings of the 39th Annual Conference of the Association for Computer Aided Design in Architecture (ACADIA). Austin, Texas, USA: ACADIA. https://papers.cumincad.org/cgi-bin/work s/paper/acadia19_576.

Skylar-Scott, Mark A, Jochen Mueller, Claas W Visser, and Jennifer A Lewis. 2019. "Voxelated soft matter via multimaterial multinozzle 3D printing." Nature 575 (7782): 330–335.

Sodupe-Ortega, Enrique, Andres Sanz-Garcia, Alpha Pernia-Espinoza, and Carmen Escobedo-Lucea. 2018. "Accurate calibration in multi-material 3D bioprinting for tissue engineering." Materials 11 (8): 1402.

Song, Haichuan, Jonàs Martínez, Pierre Bedell, Noémie Vennin, and Sylvain Lefebvre. 2019. "Colored fused filament fabrication." ACM Transactions on Graphics (TOG) 38 (5): 1–11.

Sridharan, Srinivasan. 2008. Delamination behaviour of composites. Elsevier.

Sun, Jingting, Jianzhuang Xiao, Zhengrong Li, and Xiwen Feng. 2021. "Experimental study on the thermal performance of a 3D printed concrete prototype building." Energy and Buildings 241:110965.

Yin, Jun, Chaohua Lu, Jianzhong Fu, Yong Huang, and Yixiong Zheng. 2018. "Interfacial bonding during multi-material fused deposition modeling (FDM) process due to inter-molecular diffusion." Materials & Design 150:104–112.

IMAGE CREDITS

All other drawings and images by the authors.

Teng Teng is a Ph.D. candidate at the University of Pennsylvania and a member of the Polyhedral Structures Laboratory (PSL). His work focuses on advanced manufacturing methods and tools, aiming to merge design and fabrication to create innovative and efficient production techniques. His research spans mechatronics, robotics, advanced manufacturing, and materials science.

Yefan Zhi is a second-year Ph.D. student in Architecture at the University of Pennsylvania. His research optimizes the energy and material efficiency of architectural structures from a design-for-manufacturing perspective. His work extensively exploits computational geometry and graph algorithms for automating fabrication rationalization and enabling fabrication-oriented design.

Masoud Akbarzadeh is an Associate Professor of Architecture in Structures and Advanced Technologies and the Director of the Polyhedral Structures Laboratory (PSL) at the University of Pennsylvania. His research focuses on Three-Dimensional Graphic Statics, an innovative geometric approach to structural design in three dimensions. In 2020, he was awarded the National Science Foundation (NSF) CAREER Award to further develop 3D/Polyhedral Graphic Statics methods for education, design, and the optimization of high-performance structures.